

DeepMapping: The Case for Learned Data Mapping for Compression and Efficient Query Processing

Lixi Zhou
Arizona State University
Tempe, USA
lixizhou@asu.edu

Selcuk Candan
Arizona State University
Tempe, USA
candan@asu.edu

Jia Zou
Arizona State University
Tempe, USA
jia.zou@asu.edu

ABSTRACT

Storing tabular data in a way that balances storage and query efficiencies is a long standing research question in the database community. While there are several lossless compression techniques in the literature, in this work we argue and show that a novel *Deep Learned Data Mapping (or DeepMapping)* abstraction, which relies on the impressive *memorization* capabilities of deep neural networks, can provide better storage cost, better latency, and better run-time memory footprint, all at the same time. Our proposed DeepMapping abstraction transforms a data set into multiple key-value mappings and constructs a multi-tasking neural network model that outputs the corresponding *values* for a given input *key*. In order to deal with the memorization errors, DeepMapping couples the learned neural network with a light-weight auxiliary data structure capable of correcting errors. The auxiliary structure further enables DeepMapping to efficiently deal with insertions, deletions, and updates, without having to re-train the mapping. Since the shape of the network has a significant impact on the overall size of the DeepMapping structure, we further propose a multi-task hybrid architecture search strategy to identify DeepMapping architectures that strike a desirable balance among memorization capacity, size, and efficiency. Extensive experiments with synthetic and benchmark datasets, including TPC-H and TPC-DS, demonstrated that the proposed DeepMapping approach can significantly reduce the latency of the key-based queries, while simultaneously improving both offline and run-time storage requirements against several cutting-edge competitors.

ACM Reference Format:

Lixi Zhou, Selcuk Candan, and Jia Zou. 2018. DeepMapping: The Case for Learned Data Mapping for Compression and Efficient Query Processing. In *Proceedings of ACM Conference (Conference'17)*. ACM, New York, NY, USA, 13 pages. <https://doi.org/10.1145/1122445.1122456>

1 INTRODUCTION

Real-time computations are increasingly pushed to edge servers that have limited computational and storage capabilities compared to cloud environments. In-memory computing is also popular on edge platforms to ensure real-time response. As a result, it is critical

Permission to make digital or hard copies of all or part of this work for personal or classroom use is granted without fee provided that copies are not made or distributed for profit or commercial advantage and that copies bear this notice and the full citation on the first page. Copyrights for components of this work owned by others than ACM must be honored. Abstracting with credit is permitted. To copy otherwise, or republish, to post on servers or to redistribute to lists, requires prior specific permission and/or a fee. Request permissions from permissions@acm.org.
Conference'17, July 2017, Washington, DC, USA

© 2018 Association for Computing Machinery.
ACM ISBN 978-x-xxxx-xxxx-YY/MM... \$15.00
<https://doi.org/10.1145/1122445.1122456>

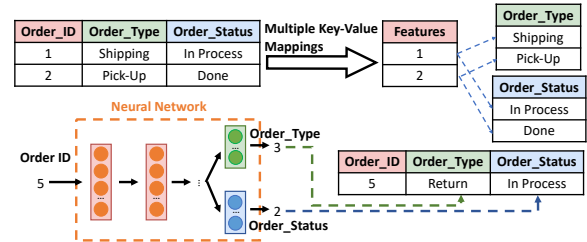


Figure 1: DeepMapping relies on neural networks to memorize key-value mapping in tabular data

to balance storage (e.g., disk size, memory footprint) and computational costs (e.g., query execution latency) on these platforms. However, existing solutions are not sufficiently effective in integrating compression and indexing techniques to achieve low storage costs and low query latency at the same time: (de)compression operations are usually computational-intensive and indexing techniques impose additional overheads for storing the indexing structure.

In this work, we argue for a novel data abstraction, called *Deep Learned Data Mapping (or DeepMapping)*, which leverages deep neural networks to seamlessly integrate the compression and indexing capabilities. This is illustrated in Figure 1 with a sample scenario, where a tabular Orders dataset is represented as two mappings from the key Order_ID to the attributes Order_Type and Order_Status, respectively. In DeepMapping, these two mappings are stored as one multi-tasking neural network which takes Order_ID as input feature and outputs Order_Type and Order_Status as labels.

As we show in the paper, DeepMapping achieves better storage cost and runtime latency at the same time, with one-time, fully automated model search and training. Most importantly, DeepMapping achieves *zero* accuracy loss and provides flexibility in query/s-can/update/insertion/deletion using a novel auxiliary structure. The proposed DeepMapping abstraction can potentially be applied to a broad class of database problems that rely on the key-value data, such as hash maps that are used in hash-based join and aggregation, and key-value stores, a critical component of modern data management and processing platforms¹.

1.1 Opportunities in Learned Data Mapping

As outlined above, this work explores the possibility of leveraging the impressive memorization capabilities of neural networks [53] for *key-value based maps* for compression and efficient query processing. In developing DeepMapping, we are motivated by several opportunities brought by deep neural network models:

- **Compressibility for size reduction.** Deep learning models usually have significantly smaller sizes compared to its training

¹While DeepMapping can also support more complex data operations such as join and aggregation, we leave the investigation of complex query processing as future work.

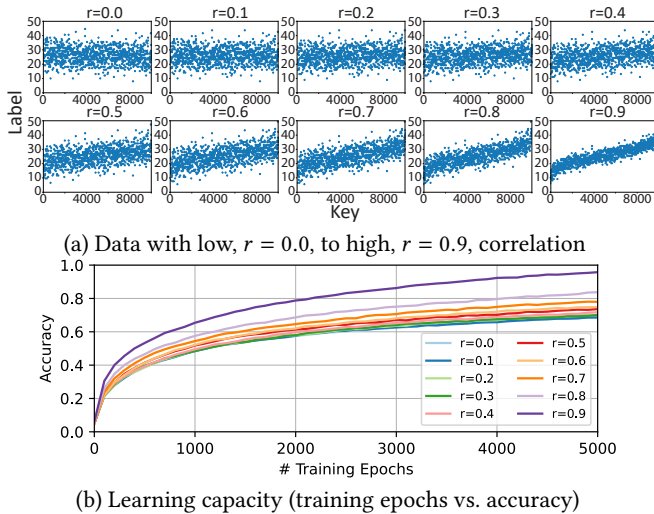


Figure 2: Learning capacity of a 2-layer fully-connected neural network for data with different statistical properties

datasets. For example, the common crawl data set has 2.6 billion of tuples and is 220 Terabytes in size [38], yet the embedding model trained on this dataset, using the language-agnostic BERT sentence embedding model, is just 1.63 Gigabytes in size [5, 11]. This provides opportunities for significant gains in storage complexities. Naturally, however, compressibility is a function of the statistical properties of the data, such as the underlying key-value correlations (Figure 2). In this work, we investigate how these affect the resulting model size.

• **Hardware acceleration opportunities.** In general, (batched) inference computations of a neural network can be accelerated using hardware such as Graphics Processing Units (GPU) processors, particularly for large-scale models and large batches. This provides opportunities for significantly improving the query throughput.

While there exist related works exploiting these opportunities for efficient indexing, approximate query processing, and compression (See Section 2), DeepMapping are facing *unique* challenges.

1.2 Challenges

• **Accuracy.** Although the universal approximation theorem [12, 22, 23] states that given a continuous function defined on a certain domain, even a neural network with a single hidden layer can approximate this continuous function to arbitrary precision, it is difficult to derive a tight bound for the accuracy of the learned data mapping [49]. Moreover, many database applications in production do not accept approximate query results [35]. So the first challenge is *to provide 100% accurate query results.*

• **Updates.** Although simple key-based queries, such as `SELECT Order_Type FROM Orders WHERE Order_ID=1`, can be implemented as inference operations over neural models, it is not straightforward to implement update, insertion, deletion. Particularly, relying on incremental model (un)learning for above operations can result in "catastrophic forgetting" issues [33]. Moreover, retraining the model upon every batch of modification is also infeasible due to the non-trivial training overheads. So the second challenge is *to implement modification queries.*

• **Model Search.** The memorization performance of the DeepMapping depends on the underlying neural network model. Obviously, it would be difficult and laborious for developers to manually search for architectures to replace tabular data. Therefore, the third critical challenge is *to automate and optimize the model search process.*

These challenges are formalized as desiderata in Section 3.

1.3 Our Contributions: DeepMapping

To address these challenges, we introduce a novel DeepMapping approach, outlined in Figure 3 (and detailed in Section 4).

(1) **A Novel Hybrid Data Representation (Sec. 4.2)** As outlined above, a relatively simple neural network can often memorize a large portion of the data, but achieving the last-mile accuracy requires a large and complicated model [26], which can be counter-productive for our purposes. Moreover, when querying non-existing data, a neural network may be incapable of telling whether this record exists or not. To tackle these challenges, instead of trying to increase the model size to achieve the last-mile accuracy, we propose to couple a relatively simple and imperfect neural network with a light-weight auxiliary structure that manages the mis-classified data and maintains an existence indexing:

- *A Compact, Multi-Task Neural Network Model* trained to capture the correlations between the key (i.e. input features) and the values (i.e. labels) of a given key-value data set. To memorize the data with multiple attributes, we propose to train a multi-task neural network, where each output layer outputs the value for its corresponding attribute. The query answering process is implemented through batch inference, where the model takes a (batch of) query key(s) as input, and outputs the predicted value(s).

- *An Auxiliary Accuracy Assurance Structure* compresses the part of the mappings that are *mis-classified* by the model, as well as a compact snapshot of the keys, to ensure the query accuracy. While the neural network memorizes most of the data, the auxiliary data structure memorizes a small amount of mis-classified data to achieve 100% overall accuracy on data query; an additional bit vector is used to record the existence of the data, which can also be leveraged to implement insertion, deletion, and updates.

(2) **Multi-Task Hybrid Architecture Search (MHAS) (Sec. 4.3)**

In order to meet the compression and latency performance desiderata, to be formalized in Section 3, the hybrid architecture needs to meet a set of goals: (a) The architecture should maximize the sharing of model layers/parameters across the inference tasks corresponding to different mappings. (b) The model should specialize well for tables with attributes that have heterogeneous types and different distributions. To help identify an effective hybrid architecture, we propose a directed acyclic graph (DAG) abstraction of the search space and a learning based multi-task search strategy that adaptively tunes the number of shared layers and private layers to balance the sharing of parameters across inference tasks, while simultaneously supporting specialization for each task.

(3) **Workflows for Insertions, Deletions, and Updates (Sec. 4.4)**

To address the challenge of supporting data modifications, we propose a lazy-update process which re-purposes the light-weight auxiliary structure outlined above by *materializing the modification*

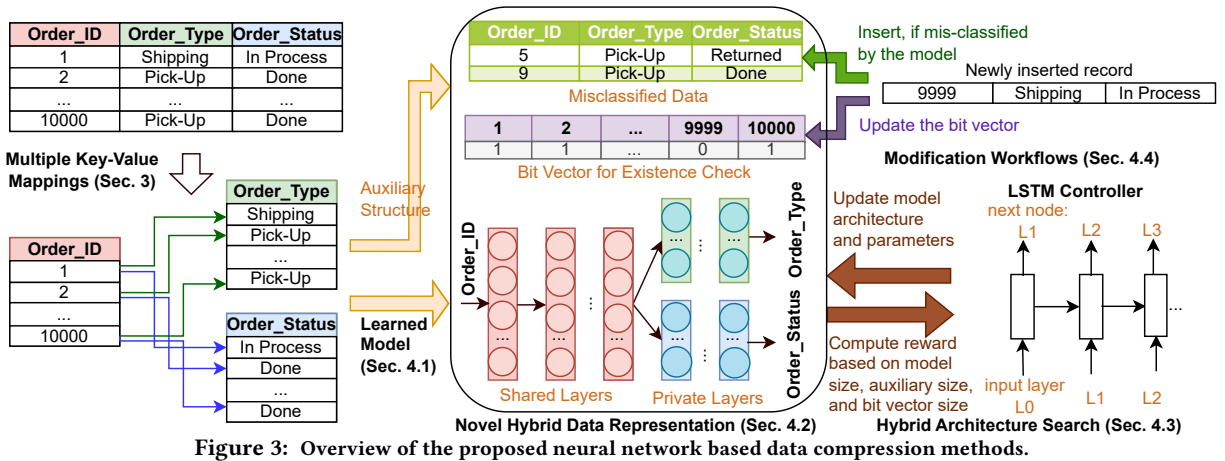


Figure 3: Overview of the proposed neural network based data compression methods.

operations in this structure, if the model cannot capture those modifications. The system triggers retraining of the neural network model only when the size of the auxiliary structure exceeds a threshold.

Other Data Operations. While, in this paper, we focus on mapping and data updates, we note that the proposed data structure can also support more complex operations. For example, scans can be implemented efficiently by running a batch inference over the samples in a given key range and then the existence index can be used to prune the inference results. We leave the investigation of more complex data operations and query processing as future work.

We implemented the proposed approach and assessed its effectiveness in various contexts. We have conducted extensive experiments with synthetic and benchmark datasets, including TPC-H and TPC-DS. The evaluation results demonstrated that the proposed DeepMapping approach provides a better balance among memorization capacity, size, and efficiency against several cutting-edge competitors, such as Z-Standard [10], Run-Length-Encoding (RLE) [16], LZ0 [3], Domain-Guided Prefix Suppression (DGPS) [17], Byte Dictionary [1], and Delta Compression (DComp) [2]. It significantly reduces the latency of the key-value mapping queries, while simultaneously improving both offline and run-time storage requirements.

2 RELATED WORKS

Learned Indexing. Driven by the desirable properties of the neural networks outlined in Section 1.1, in recent years, several deep learning based techniques, commonly known as *learned index* structures [13–15, 25, 26, 28, 36, 37, 40], have been proposed to improve the computational efficiency of indexing structures. These techniques apply machine learning to capture the correlation between the keys and the positions of the queried values in underlying storage. There also exist works [19, 42–44] that use a machine learning model to replace the hash function for hash indexing. While these techniques achieved better storage and query efficiency compared to existing indexing techniques, the problem we target in this paper is different from learned indexes in several critical ways:

- Generally speaking, learned indexing predicts positions in a (sorted) array, which is commonly posed as a regression task. We, however, are aiming to learn a direct key-value mapping – moreover, the values can be discrete or categorical.

- For learned indexing, if the queried value is not found in the predicted position, the search can continue, as usual, on the (sorted) array until the value is found or determined as non-existing. This is not possible for learning a direct key-value mapping.
- Learned indexing only compresses the indexing structure, but will not compress the data. This is a key difference with our proposed technique, which combines both lossless data compression and indexing and strikes an even better trade-off among overall storage efficiency and retrieval efficiency.

Learned Approximate Query Processing (AQP). Recent works [20, 32, 47, 48] applied learning-based techniques to improve AQP or AQP with differential privacy [47]. Their solution and theoretical bounds only work for range aggregation queries. Different from their works, we focus on lossless query processing by leveraging a novel auxiliary structure that manages mis-classified data. While this work focuses on key-based look-up queries, it is easily extensible to more complicated queries. For example, a scan operation can be performed as a batch inference based on the existence index. The key-based join and aggregation queries can also use our hybrid structure as a hash-table.

Compression. Abundant works [24, 34, 46] focus on the lossless compression of high-dimensional data using a deep learning approach. The idea is to choose a statistical model that closely captures the underlying distribution of the input data and develop a scalable compression/encoding algorithm that exploits the statistical model. These works do not maintain the key-value mappings and it thus cannot accelerate the queries on top of the data. Different from these works, our work focuses on balancing the data compression ratio and data retrieving efficiency.

3 PROBLEM AND DESIDERATA

We first formulate the problem and desiderata as follows:

- **Single-Relation, Single-Key Mapping.** In a relation, a key may consist of multiple attributes. Let $R(K_1, \dots, K_l, V_1, \dots, V_m)$ be a relation where $K = (K_1, \dots, K_l)$ represents a key that consists of l attributes and V_1 through V_m are m value attributes. The goal is to identify a mapping data structure, $d_\mu()$ which, given a key $\mathbf{k} = (k_1, \dots, k_l) \in \text{domain}(K)$, and a target attribute $V_i \in \{V_1, \dots, V_m\}$, it returns $d_\mu(\mathbf{k}, V_i) = \pi_{V_i}(\sigma_{K_1=k_1 \wedge \dots \wedge K_l=k_l}(R))$. In

this work, due to space limit, we focus on this problem, while our approach is extensible to the following two problems.

- **Single-Relation, Multiple-Key Mapping.** Note that in practice a relation may have multiple candidate keys in addition to the primary key, and it may contain one or more foreign keys with each foreign key linking to the primary key of another table. We further represent the collection of keys as $\mathcal{K} = (\mathcal{K}^1, \dots, \mathcal{K}^S)$. Therefore, we more generally seek a multiple-mapping data structure, $d_\mu()$ which takes a key $\mathbf{k}^i = (k_1, \dots, k_l) \in \text{domain}(\mathcal{K}^i \in \mathcal{K})$ along with a target value attribute $V_j \in \{V_1, \dots, V_m\}$, it returns $d_\mu(\mathbf{k}^i, V_j) = \pi_{V_j}(\sigma_{\mathcal{K}_1^i=k_1 \wedge \dots \wedge \mathcal{K}_l^i=k_l}(R))$.
- **Multiple-Relation, Multiple-Key Mapping.** Furthermore, in many contexts, such as databases with star schemas, the same attribute can serve as key for one relation (e.g., the fact table) and serve as foreign key for other relations (e.g., the dimension tables). Let us consider $\mathcal{R} = \{R_1, \dots, R_r\}$ be a set of relations. In this case, we seek a multiple-mapping data structure, $d_\mu()$, which takes a key $\mathbf{k}^i = (k_1, \dots, k_l) \in \text{domain}(\mathcal{K}^i \in \mathcal{K})$, a target value attribute $V_j \in \{V_1, \dots, V_m\}$, along with a target relation $R_u \in \mathcal{R}$, and it returns $d_\mu(\mathbf{k}^i, V_j, R_u) = \pi_{V_j}(\sigma_{\mathcal{K}_1^i=k_1 \wedge \dots \wedge \mathcal{K}_l^i=k_l}(R_u))$.

For any of these three alternative problem scenarios, our key desiderata from the mapping data structure, $d_\mu()$, are as follows:

- **Desideratum #1 - Accuracy:** $d_\mu()$ is accurate – i.e., it does not miss any data and it does not return any spurious results.
- **Desideratum #2 - Compressibility:** The offline disk storage space and runtime memory footprint of $d_\mu()$ structure are small.
- **Desideratum #3 - Low latency:** The data structure $d_\mu()$ is efficient and, thus, provides low data retrieval latency.
- **Desideratum #4 - Updateability:** $d_\mu()$ is updateable with insertions of new key-value rows and deletions of some existing keys from the database. Moreover, the data structure also allows changing the value of an existing key.

4 DEEPMAPPING ARCHITECTURE

In DeepMapping, we encode the mapping from each key to each column as an inference task leveraging a neural network model that predicts, given a key, the corresponding column as label.

4.1 Shared Multi-Task Network

In this paper, we are targeting key-value mappings where the key and values are discrete, such as integers, strings, categorical values. Without loss of generality, we consider a sequence of fully connected layers as the underlying neural network architecture, where the strings or categorical data are encoded as integers using one-hot encoding before training and inference.

In order to achieve high compression rates, some of these layers can be shared across multiple inference tasks within a relation and across relations that have foreign key reference relationships. At the same time, other layers may be private to each individual inference task to improve the accuracy of that particular inference task. Considering the example as illustrated in Figure 1, we train a multi-layer fully connected neural network with two output layers, one for the Order_Type column and the other for the Order_Status column, respectively. The first few layers of the neural network, which capture the structures common to both inference tasks, are shared; the latter layers of the neural network, which capture the

output attribute specific structures, on the other hand are private to specialize the network for each individual output attribute.

4.2 Ensuring 100% Accuracy (Desideratum #1)

The first and the most important, of our four desiderata, listed in Section 3, is *accuracy*: i.e., DeepMapping should not miss any data and should not return spurious results.

Why not simply try to overfit the data? As we discussed earlier, in theory (by the universal approximation theorem [12, 22]) a sufficiently large network should be able to perfectly memorize and given data. In most machine learning applications, this is referred to as *overfitting* and is in fact undesirable:

- A model that is overfitting is often unnecessarily large (and hence expensive to train and infer). In order to achieve the last-mile accuracy, e.g., to improve the accuracy from 90% to 100%, the required neural network model size will significantly increase, often by multiple times [26].
- Models that are overfitting often do not generalize to unseen data, which makes them ineffective in generalizing to the prediction tasks for insertions.

Therefore, seeking an arbitrarily large model to achieve 100% accuracy is not appropriate, considering the desiderata include updateability, compressibility and low latency.

Can we prevent models from hallucinating when a key is missing? In addition, when querying the non-existing data, it is challenging for the neural networks to accurately tell whether the tuple exists or not. This is because, the inference task will *predict* an output even when the data is not seen in the input – this makes the neural network based solutions useful for generalizing, but in our context, any such output will be spurious and will need to be avoided, as a *hallucination*.

Solution: Lightweight auxiliary Accuracy Assurance Structures. To address these issues, we propose to use a novel *hybrid data representation*, consisting of (1) a compact *neural network model* that memorizes the data (denoted as M), (2) an *auxiliary accuracy assurance* table (denoted as T_{aux}) that compresses any misclassified data, and (3) an *existence bit vector* (denoted as V_{exist}), whose range corresponds to the key range – intuitively, each bit marks the existence of the corresponding key.

4.2.1 Encoding of the Auxiliary Structures. The *auxiliary accuracy assurance* table, T_{aux} , is filled by running all the keys in the input key-value mapping through the trained model and checking whether the inferred result is matching the correct output values – if not (i.e., if the key-value mapping is mis-learned) the corresponding key-value pair is stored in the auxiliary table. The mis-learned key-value pairs are sorted by the key, the domain of keys is equally partitioned into p partitions, and each mis-learned key-value pair is stored in the corresponding partition in sorted order. To further reduce the storage overhead, we apply Z-standard compression [10] on each partition before they are stored. In this work, we focus on keys that consist of integers and use a single dynamic bit array to serve an existence index for the keys, denoted as V_{exist} , where It is also compressed using Z-standard [10]. In addition, the decoding

Algorithm 1 (Parallel) Batch Key Lookup by DeepMapping

```

1: INPUT:
    $Q$ : A vector of  $k$  encoded query keys.
    $M$ : Pre-trained neural network.
    $T_{aux}$ : Auxiliary table that stores the mis-classified data.
    $V_{exist}$ : Bit vector for existence check.
    $f_{decode}$ : Decoding map.
2: OUTPUT:  $R$ : A vector of  $n$  queried values.
3:  $R = M.infer(Q)$  // running in GPU as batch inference
4: for  $i = 1$  to  $n$  do
5:   if  $V_{exist}[Q[i]] == 1$  then
6:     if  $Q[i]$  exists in  $T_{aux}$  then
7:        $R[i] = T_{aux}[Q[i]]$ 
8:     end if
9:   else
10:     $R[i] = NULL$ 
11:  end if
12: end for
13:  $R = f_{decode}(R)$  // decoding
14: return  $R$ 

```

map (denoted as f_{decode}) that converts predicted labels from an integer codes (resulted from one-hot encoding) to its original format, is also part of the auxiliary structure.

4.2.2 Lookup Process. The look-up process using the proposed hybrid data representation is illustrated in Algorithm 1 - the key aspects of the process are outlined below:

Inference. DeepMapping allows for simultaneous querying of a batch of encoded keys, leveraging parallel inference using the GPU.

Existence check. While the GPU is busy with the inference, we simultaneously check, using the CPU, the existence of each query key in the V_{exist} data structure to eliminate any spurious results.

Validation. For any key that passes the existence check, we check using CPU the auxiliary table, T_{aux} , to see whether this key was mis-learned by the model. To look up the query key in the auxiliary table, we first locate its partition, bring it to the main memory, and decompress it; we then apply a binary search to look up the value within the partition. If the query key is located in the auxiliary table, it means that the key-value pair was mis-learned by the model and we return the value from the auxiliary table. Otherwise, the model's output is returned as the result. Note that we provide two different strategies to handle the decompression of the partitions (line no.6 in Algorithm 1) to facilitate the validation process:

- *Memory-optimized validation strategy.* In memory constrained devices, we free up the space of the last decompressed partition before bringing the next partition of the auxiliary table to memory in order to keep the run-time memory usage low. In this case, query keys in a batch are sorted before validation so that each partition is decompressed only once for each query batch.
- *Latency-optimized validation strategy.* The latency-efficient strategy caches all the decompressed partitions of the auxiliary table. These cached partitions can be used for future queries and this would eliminate the need to read the partitions from secondary storage and decompress them. This reduces the lookup times, but requires more memory for caching.

Note that, while their primary benefit is to ensure 100% accuracy without necessitating a prohibitively large model, as

we see in Section 4.4, these auxiliary structures also enable insert/update/delete operations on the data.

4.3 Multi-Task Hybrid Architecture Search (MHAS) (Desiderata #2, 3)

A critical part of the data registration process is to select a neural network architecture to fully memorize the data while achieving the desiderata listed in Section 3. Let us be given a dataset R that consists of n tuples, where each tuple is represented as $\langle \mathbf{x}, \mathbf{y} \rangle$. Here, \mathbf{x} represents a collection of one or more attributes that serve as the key so that each key uniquely and minimally identifies a tuple. \mathbf{y} represents a collection of m attributes that are disjoint with \mathbf{x} and serve as the values. Our goal is to identify a hybrid data representation, $\hat{M} = \langle M, T_{aux}, V_{exist}, f_{decode} \rangle$, consisting of a neural network model, M along with the auxiliary structures, T_{aux} , V_{exist} , and f_{decode} , satisfying our desiderata. As aforementioned in Sec. 4.1, we consider a multi-layer fully connected neural network to memorize a significant portion of the data in the given relation(s). As depicted in Figure 1, some of layers (which help abstract the key) are shared across multiple data columns, while some others may be private to each output attribute. Therefore, the problem needs to be posed as a multi-task model search problem.

Neural architecture search is an active research area [9, 18, 27, 29, 39, 41, 50]. A key distinction of our work is that, instead of searching for a neural network, we are searching for a hybrid data structure, which as a whole achieves the key desiderata. To develop our multi-task hybrid architecture search (MHAS) strategy, we build on the *efficient neural architecture search* (ENAS) strategy [39], which supports parameter sharing across sampled model architectures. While the original motivation of this parameter sharing is to improve the efficiency of NAS by forcing all sampled child models to share weights to eschew training each model from scratch, in this paper, we argue that this approach can also help reduce the model search overhead in multi-task learning by encouraging parameter sharing across multiple tasks. Note that previous works on transfer and multi-task learning has shown that parameters learned for a model on a given task can be used for other tasks with little to no modifications [45]. This observation also underlies the current success and wide-spread use of large pre-trained models, such as large language models [31, 51, 52], across diverse tasks. In order to achieve our desideratum of identifying a *small* network well-tailored to our data, the MHAS search strategy must distinguish shareable and non-shareable layers across the different tasks.

At the surface, similar to ENAS, our MHAS strategy consists of two components: *a search space*, which defines how the components of the underlying neural network can be connected to each other to enumerate new neural architectures, and *a controller algorithm* which seeks a structure for the target model within this search space. The MHAS search algorithm, however, differs from ENAS in several ways: (a) MHAS is extended with the ability to search for multi-task models, with shareable and non-shareable layers. (b) To balance compressibility brought by shared layers and accuracy brought by the private layers, MHAS searches within a search space without fixed numbers of hidden layers among the shared layers and private layers for each task. (c) Since our goal is not to search for a neural network, but a hybrid structure, the search is governed by an objective function that captures our desiderata. We next

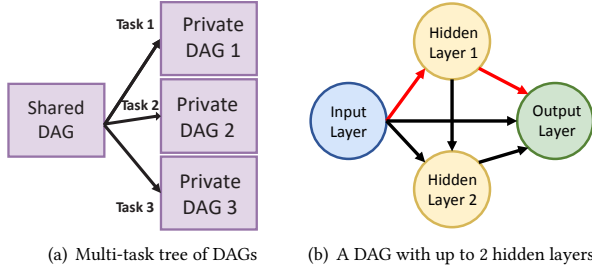


Figure 4: (a) Two-level tree representing shared and private DAGs and (b) a DAG corresponding to one of the nodes – here the subgraph connected with the red edges illustrates a sampled model with only a single hidden layer

formalize the search space used by our algorithm in Section 4.3.1 and we then present the controller algorithm in Section 4.3.2.

4.3.1 MHAS Multi-Task Search Space. We represent the search space as a two-level tree, where the root corresponds to the shared layers and each leaf represents the private layers for a target column. Figure 4(a) illustrates a high-level view of the search space of a model designed to infer a relation with three value columns. In this example, the search space consists of a tree with four nodes: one for the shared layers (capturing the characteristics of the key) and three nodes for the private layers, each corresponding to a target value column.

As we discussed earlier, in this work, as the underlying neural architecture, we consider fully-connected layers² (with different number of neurons). Each node of the tree is represented by a directed acyclic graph (DAG). A DAG contains a node representing the input layer, a node representing the output layer, and multiple nodes representing candidate hidden layers. As illustrated in Figure 4(b), the DAG represents a search space that contains up to two hidden layers. Edges of the DAG represent all possible data flows among these layers (with each edge corresponding to a specific model parameter tensor that connects the two layers). Given this, the model search process can be posed as enumerating subgraphs of the DAGs by *activating* and *deactivating* network edges – each *activated* directed edge represents a connection between two neural network layers. Deactivated edges represent connections that do not exist in that particular network. In Figure 4(b), red color is used to highlight activated edges: in the example, the subgraph represented with the red edges corresponds to a sampled model with a single hidden layer between the input and output layers.

4.3.2 Multi-Task Model Search Controller. The DeepMapping multi-task model search algorithm is outlined in Algorithm 2. Since the goal is to learn a sequence of nodes (and train the model parameters at each edge), as in ENAS [39], the DeepMapping controller is constructed as a long short-term memory (LSTM) neural network architecture. The LSTM architecture samples decisions via softmax classifiers in an autoregressive fashion to derive a sequence of nodes in the DAG. The algorithm runs over N_t iterations – at each

Algorithm 2 MHAS Model Search Algorithm

```

1: INPUT:
    $D$ : A dataset to be memorized
    $\theta$ : The controller model parameters
    $W$ : The weights of all candidate layers in the search space
    $N_t, N_m, N_c$ : The number of search, model training, and controller
   training iterations and controller training iterations
    $D_{batch}$ : batch size used in each model/controller training iteration
    $m\_epochs$ : number of epochs in each model training iteration
2: OUTPUT: optimal model structure  $M$ 
3: for  $i = 1$  to  $N_t$  do
4:   # Controller parameter  $\theta$  is fixed
5:   if  $i \bmod \lfloor \frac{N_t}{N_m} \rfloor == 0$  then
6:     # Train a sampled model for  $N_m$  iterations
7:     Sample a model  $M$  from the search space
8:     for  $k = 1$  to  $m\_epochs$  do
9:       for  $D_{batch} \in D$  do
10:        Update  $W$  through  $M.fit(D_{batch})$ 
11:       end for
12:     end for
13:   end if
14:   if  $i \bmod \lfloor \frac{N_t}{N_c} \rfloor == 0$  then
15:     # Model weight  $W$  is fixed
16:     for  $D_{batch} \in D$  do
17:       Sample a model  $M$  from the search space
18:       Update  $\theta$  through  $\mathcal{L}(M, D)$ 
19:     end for
20:   end if
21: end for
22: return  $M$ 

```

iteration, the algorithm alternatively trains the controller parameter θ in a *controller training iteration* or the weights of the sampled neural architecture M through a *model training iteration*:

- During a *controller training iteration*, the weights, W , of the candidate layers in the search space is fixed. For each batch of the data, the controller samples a model from the search space and updates the controller parameter, θ , through the loss function, $\mathcal{L}(\hat{M}, D)$ (D represents the dataset to be compressed):

$$\frac{\text{size}(M) + \text{size}(T_{aux}) + \text{size}(V_{exist}) + \text{size}(f_{decode})}{\text{size}(D)}$$

The controller samples a model by taking a DAG node as input and picking the next DAG node among the ones that connect to it; the selected node serves as the input for the next iteration of the process. This process repeats until the output node is selected or the maximum number of steps have been used.

- During a *model training iteration*, DeepMapping trains the weights of the sampled neural architecture in m_epochs by fixing the controller parameters (θ). We use standard cross entropy [21] as the loss function to update model weights M . Since the sampled neural architecture is a subgraph of the search space, and these layers may be sampled again in future iterations, each model training iteration may contribute to improving the accuracy and convergence rate of future model training iterations by sharing parameters across iterations.

Note that each training iteration is ran for $\frac{\text{size}(D)}{\text{size}(D_{batch})}$ training steps. Since, the memorization task may in practice need a larger number iterations to stabilize to a desired level, usually we choose

²As we also validate through experiments, tabular data can be represented well using fully connected layers [30].

$N_m > N_c$, where N_m is the number of model training iterations and N_c is the number of controller training iterations.

4.4 DeepMapping Updates (Desideratum #4)

Neural networks are notoriously challenging to be updated: (a) incremental training tends to reduce the accuracy for existing data; (b) it is difficult to tell the neural network to forget something that is already learned; and (c) retraining incurs significant latency and thus it is often not an acceptable solution to handle updates to the data. Therefore, to support data modification operations, insert/update/delete, we piggy-back on the auxiliary structure that we have described in Section 4.2:

Insertions. Given a collection of key-value pairs (D_{insert}) to be inserted into the DeepMapping’s hybrid data structure, we first check whether the model (M) can generalize to them by running inference over the keys for the target columns. Only those key-value pairs that are incorrectly inferred need to be inserted into the auxiliary table (T_{aux}). The bit vector, V_{exist} is updated correspondingly. The insertion process is formalized in Algorithm 3.

Algorithm 3 Insert

```

1: INPUT:
    $D_{insert}$ : A collection of  $n$  tuples to be inserted.
    $M$ : The pre-trained neural network model.
    $T_{aux}$ : The auxiliary table that stores the mis-classified data.
    $V_{exist}$ : The bit vector for existence check.
2: for  $i = 1$  to  $n$  do
3:    $V_{exist}[D_{insert}[i].key] = 1$ 
4:   if  $f_{decode}(M.infer(D_{insert}[i].key)) = D_{insert}[i].values$  then
5:     continue
6:   else
7:      $T_{aux}.add(D_{insert}[i])$ 
8:   end if
9: end for

```

Deletions. The deletion process is relatively straightforward as it can be implemented simply by marking the corresponding bit as 0 in the bit vector, V_{exist} . This is illustrated in Algorithm 4.

Algorithm 4 Delete

```

1: INPUT:
    $D_{delete}$ : A collection of  $n$  keys to be deleted.
    $V_{exist}$ : A bit vector for existence check.
2: for  $i = 1$  to  $n$  do
3:    $V_{exist}[D_{delete}[i]] = 0$ 
4: end for

```

Updates. We treat updated key-value pairs (D_{update}) as mis-memorized data and insert the new values into the auxiliary table (T_{aux}). Since the keys already exist (otherwise, the process would be an insertion), we do not need to update the existence index. The process is illustrated in Algorithm 5.

DeepMapping re-trains the model and reconstruct the auxiliary structures on the underlying data to optimize the compression ratio and query efficiency, only when the auxiliary table becomes too large to satisfy the Desiderata listed in Section 3.

5 EVALUATION

We implemented the DeepMapping hybrid structure, model search, and look-up and modification query execution^{??}. In this section, we

Algorithm 5 Update

```

1: INPUT:
    $D_{update}$ : a vector of  $n$  tuples to be updated.
    $T_{aux}$ : Auxiliary table that stores the mis-classified data.
2: for  $i = 1$  to  $n$  do
3:   if  $f_{decode}(M.infer(D_{update}[i].key)) = D_{update}[i].values$  then
4:      $T_{aux}.remove(D_{update}[i])$ 
5:   else
6:     if  $D_{update}[i] \notin T_{aux}$  then
7:        $T_{aux}.add(D_{update}[i])$ 
8:     else
9:        $T_{aux}.update(D_{update}[i])$ 
10:    end if
11:  end if
12: end for

```

evaluate the effectiveness of DeepMapping using TPC-H [7], TPC-DS [6], with different scale factors (1 and 10), as well as a dataset synthesized from TPC-H and TPC-DS. Since, we are targeting data where the key consists of one or more integers and the values are categorical. We do not consider tables and columns that do not satisfy these conditions. Experiments are run under a Ubuntu 20.04 machine which is configured with 24 CPU Cores, 125 GB Memory, and 1 Nvidia-A10 GPU with 24 GB Memory.

5.1 DeepMapping Parameters

In the experiments, we use the following default configurations: (a) partition size for the auxiliary accuracy assurance table: 1MB; (b) total number of iterations (N_t) for the MHAS model search: 2000; (c) number of model training iterations (N_m): 2000; (d) number of controller training iterations (N_c): 40; and (g) latency-optimized validation strategy for decompressing partitions. We consider an MHAS search space consisting of DAGs with up to two shared hidden layers and two private hidden layers for each task. auxiliary. As in [39], the controller is constructed as a long short-term memory (LSTM) neural network, with 64 hidden units. During MHAS, the controller parameters, θ , are initialized uniformly in $\mathcal{N}(0, 0.05^2)$ and trained with Adam optimizer at a learning rate of 0.00035. Each model training iteration uses a learning rate of 0.001, decayed by a factor of 0.999. In each iteration, the model has been trained for 5 epochs with batch size of 16384; the controller is trained for 1 epoch every 50 iterations with batch size of 2048.

5.2 Competitors

We compare DeepMapping with lossless compression mechanisms, Domain-Guided Prefix Suppression (DGPS) [17], Byte Dictionary [1], Z-Standard [10], Run-Length-Encoding (RLE) [16], LZ0 [3], and Delta Compression (DComp) [2]. DeepMapping has been implemented in Python with the latest numpy, bitarray, tensorflow, pytorch, zstd libraries. For LZ0 and Z-Standard, we used public software [4, 8]. Others were implemented by our team using the software platform as DeepMapping. To be consistent, we set the partition size to be compressed to 1MB for all algorithms.

5.3 Query Generation and Evaluation Criteria

The evaluation criteria considered in this Section are selected based on the Desiderata listed in Section 3.

• **Latency and Storage** We consider the size of the key-value map on the disk, including the neural network model size and the size of the lightweight auxiliary table, and the run-time memory requirements. We also consider end-to-end latency for data querying.

Latency and run-time memory usage are measured by considering 5 queries, each looking up B randomly selected keys.

• **Data Manipulation** (1) update and delete: For these cases, we randomly select $X\%$ of data for revision. (2) insert: For insertions, we put aside $Y\%$ of the data, such that $(Y \times 100)/(100 - Y) = X$; after the remaining $(100 - Y)\%$ data is stored in DeepMapping, the data that were put aside are then inserted into DeepMapping (this corresponds to an $X\%$ data insertion).

• **Neural Architecture Search** We also ran a set of experiments to establish the effectiveness of the proposed MHAS strategy.

5.4 Evaluation Results

5.4.1 High-level Overview of Storage vs. Latency Trade-Off. Before presenting a detailed analysis of DeepMapping, we first provide an overview of the offline storage and end-to-end latency trade-offs.

First, in order to understand the effectiveness of DeepMapping under different configurations, we create synthesized datasets by sampling single/multiple column tables with low/high key correlations, of different sizes (100M, 1GB, 10GB) from the TPC-H and TPC-DS benchmarks. For each configuration, we measure the compressed key-value map size and end-end latency of various queries in DeepMapping and compare them against the uncompressed baseline and an alternative baseline, Z-Standard (which, as we later see in the detailed experiments, is the best performing competitor among all the competitors considered). As we see in Figure 5,

- DeepMapping provides highest benefits for large data sets, especially when there is relatively high correlation between the key and values, and
- while DeepMapping is slower than uncompressed data for large data with low key-value correlation, in all considered cases, DeepMapping provides a very high compression ratio, easily outperforming Z-standard in terms of storage-latency trade-off.

In Figures 6 through 8, we provide a more detailed comparisons of the offline storage and end-to-end latency trade-offs for various baseline/competitor algorithms for TPC-H and TPC-DS benchmark data and for different data scales and query workloads. These results demonstrate that the DeepMapping algorithm provides the best trade-off among all competitors for all scenarios – this is true except for an outlier case (TPC-DS item data with scale factor 1), where the data is very small (only 0.19MB); in this case, while it provides the best overall latency, DeepMapping is not able to provide a competitive compression rate as we see Figure 8(a).

5.4.2 Offline and Online Storage. Table 1 provides a summary of the offline storage requirements of different competitors for the TPC-H benchmark, with scale factors 1 and 10. As we see in the table, DeepMapping generally provides the best overall compression, especially for the larger scenario (scale 10). As aforementioned, among the baselines, Z-Standard is the best competitor, especially for smaller datasets, such as customer and part tables, with scale

³In the figures, uncompressed data is always at the point (1.0, 1.0). Note that, generally speaking, configurations closer to (0.0, 0.0) are more desirable in terms of compression ratios and latencies. The dashed arc, \curvearrowright , indicates the points in the space with the same L_2 distance to (0.0, 0.0) as the DeepMapping algorithm – hence configurations outside of this arc have a less desirable compression/latency trade-off than DeepMapping; the \rightarrow indicates cases where the access latency is more than $3\times$ slower than accessing the uncompressed data

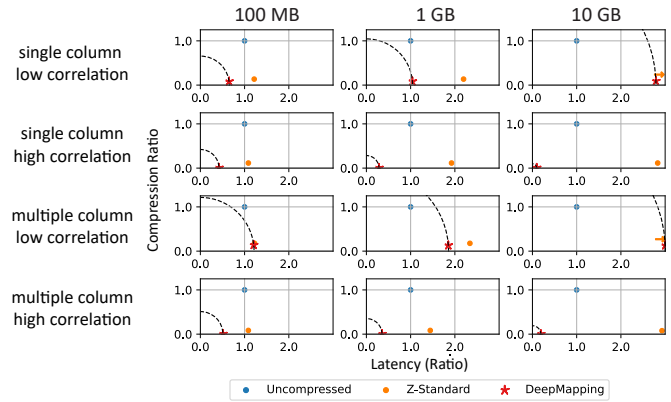


Figure 5: Trade-off between compression ratio and lookup latency for the synthetic dataset sampled from TPC-H and TPC-DS. Annotations are explained in the footnote ³

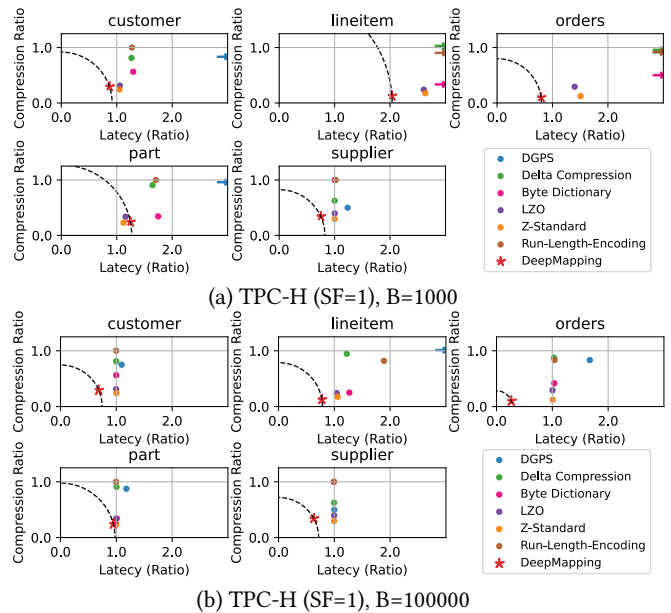


Figure 6: Trade-off between compression ratio and lookup performance for TPC-H (SF=1), B=1000 and 100000 – Annotations are explained in the footnote ³.

factor 1. In Table 2, we see that DeepMapping consistently provides the best or second best compression, especially for benchmark data with larger scale factors. Note that in the TPC-DS benchmark, there are more columns with large cardinalities (larger than 20). A consequence of this is that the memorization is somewhat harder and consequently, TPC-DS is generally harder to compress than the TPC-H data set. In contrast, the catalog_page (CP) and customer_demographics (CD) columns have very strong correlations with the key column and this makes these particular maps relatively easy to compress. Overall, these tables show that the proposed DeepMapping approach can provide significant data size reductions, with an average value of 70.8% on the considered data sets compared to the uncompressed key-map data size.

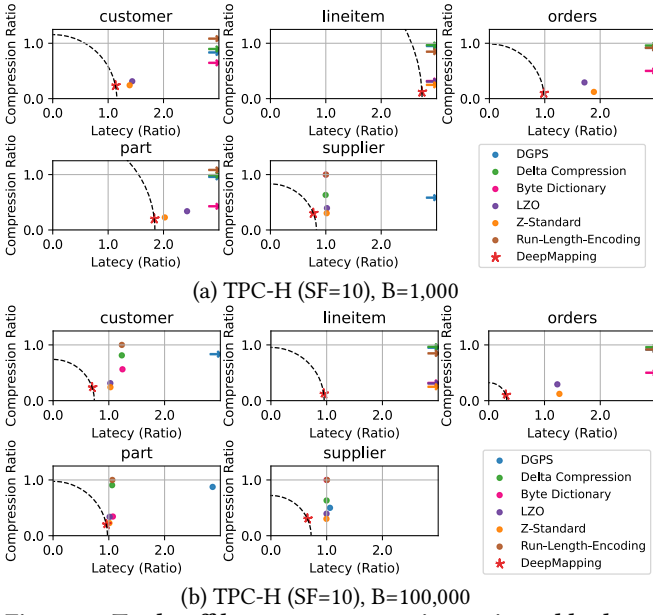


Figure 7: Trade-off between compression ratio and lookup performance in TPC-H (SF=10), B=1000 and 100000 – Annotations are explained in the footnote ³.

Table 1: Comparison of the storage overhead of using different compression mechanisms on TPC-H dataset (MB), Scale Factors: 10 and 1 – bold entry indicates the best solution, the underlined entry indicates the second best

Table Size (MB) – TPC-H, Scale Factor:10					
Methods	customer	lineitem	orders	part	supplier
Uncompressed	22.89	3432.54	343.37	61.04	0.76
DGPS	17.17	2974.97	286.17	53.41	0.38
DComp	18.60	3032.69	300.54	55.32	0.48
Byte Dictionary	12.88	801.71	143.22	20.99	0.76
LZO	7.18	771.23	100.57	20.68	0.30
RLE	22.89	2623.87	286.24	61.04	0.76
Z-Standard	5.53	<u>568.22</u>	41.78	13.84	0.234
DeepMapping	5.42	417.88	34.46	12.35	0.229

Table Size (MB) – TPC-H, Scale Factor:1					
Methods	customer	lineitem	orders	part	supplier
Uncompressed	2.29	320.50	34.34	6.10	0.08
DGPS	1.72	297.63	28.62	5.34	0.04
Delta Compression	1.86	303.40	30.05	5.53	0.05
Byte Dictionary	1.29	80.21	14.32	2.10	0.08
LZO	0.72	77.20	10.06	2.06	0.03
RLE	2.29	262.47	28.62	6.10	0.08
Z-Standard	0.55	56.31	<u>4.24</u>	1.40	0.022
DeepMapping	<u>0.67</u>	41.05	3.44	1.48	0.0261

Figures 9 and 10 provide detailed breakdown of the DeepMapping storage mechanism for TPC-H and TPC-DS data sets for different scale factors. As we see in these charts, in most of the scenarios, the bulk of the storage taken by the auxiliary table, which justifies our MHAS search algorithm, which not only considers the neural network size, but the entire size of the hybrid architecture.

³Size of decoding map is included in auxiliary table.

Table 2: Comparison of the storage overhead of using different compression mechanisms on TPC-DS dataset (MB), Scale Factors: 10 and 1 – bold entry indicates the best solution, the underlined entry indicates the second best

CP: catalog_page; CR: catalog_returns; CS: catalog_sales; CA: customer_address
 CD: customer_demographics; C: customer; I: item; SR: store_returns; WR: web_returns

Table Size (MB) – TPC-DS, Scale Factor:10									
Methods	CP	CR	CS	CA	CD	C	I	SR	WR
Uncompressed	0.23	26.40	217.83	7.20	95.25	12.47	0.93	21.17	5.24
DGPS	0.23	10.56	108.92	6.30	73.28	8.91	0.93	10.59	2.62
DComp	0.23	10.56	95.31	6.52	80.62	9.80	0.97	13.23	3.27
Byte Dictionary	0.15	26.40	217.86	4.05	16.42	6.24	0.45	21.17	5.24
LZO	0.05	11.90	94.36	1.92	6.07	4.30	0.26	8.75	2.16
RLE	0.05	26.40	174.58	5.40	12.48	12.05	0.15	21.17	5.24
Z-Standard	<u>0.01</u>	8.18	59.48	1.03	35.41	<u>2.50</u>	0.15	<u>7.34</u>	1.81
DeepMapping	0.002	8.44	68.38	0.98	0.50	2.54	0.18	7.20	1.80

Table Size (MB) – TPC-DS, Scale Factor:1									
Methods	CP	CR	CS	CA	CD	C	I	SR	WR
Uncompressed	0.22	2.64	21.81	1.44	95.26	2.50	0.19	3.12	0.52
DGPS	0.22	1.06	5.45	1.26	73.28	1.78	0.16	1.04	0.26
DComp	0.22	1.06	9.54	0.81	80.62	1.96	0.17	1.56	0.33
Byte Dictionary	0.14	2.64	21.81	0.38	43.99	1.25	0.08	3.12	0.52
LZO	0.04	1.16	9.09	0.38	16.42	0.84	<u>0.05</u>	1.31	0.21
RLE	0.04	2.58	17.17	1.08	35.41	2.36	0.16	3.12	0.52
Z-Standard	<u>0.01</u>	0.75	5.45	0.21	<u>6.67</u>	0.50	0.03	0.90	0.17
DeepMapping	0.004	0.76	5.45	0.22	0.32	0.69	0.47	0.92	0.17

Table 3: Comparison of the end-end lookup latency of using different compression mechanisms on TPC-H (ms)

Lookup time (ms) Scale Factor: 1, B=1000					
Methods	customer	lineitem	orders	part	supplier
Uncompressed	79.28	244.22	83.82	61.16	73.34
DGPS	358.38	12866.68	2351.94	1167.20	90.58
DComp	100.41	2119.81	326.81	100.68	73.38
Byte Dictionary	102.86	2438.91	361.81	106.85	73.55
LZO	83.81	637.16	117.31	70.91	73.53
RLE	100.88	7435.38	392.32	104.32	74.77
Z-Standard	83.12	643.76	126.41	68.63	73.49
DeepMapping	68.87	<u>496.54</u>	66.51	<u>76.22</u>	55.06

Lookup time (ms), Scale Factor: 1, B=100,000					
Methods	customer	lineitem	orders	part	supplier
Uncompressed	7770.41	8251.19	7202.52	5899.15	7250.79
DGPS	8513.19	40067.66	12042.04	6959.15	7250.06
DComp	7751.26	10088.28	7415.68	5922.22	7220.81
Byte Dictionary	7749.04	10474.74	7450.36	5943.70	<u>7185.96</u>
LZO	7742.90	8612.91	7228.84	5868.64	7221.86
RLE	7754.65	15589.44	7495.34	5864.76	7220.78
Z-Standard	7774.59	8735.21	7239.89	5856.49	7225.54
DeepMapping	5322.91	6403.12	1905.07	5587.14	4583.55

Lookup time (ms), Scale Factor: 10, B=100,000					
Methods	customer	lineitem	orders	part	supplier
Uncompressed	<u>7782.68</u>	<u>11102.67</u>	7666.93	5960.09	7793.17
DGPS	48095.32	1747189.40	264413.92	17055.47	8255.62
DComp	9595.02	193922.89	31098.97	6309.85	7783.29
Byte Dictionary	9687.91	209815.66	32757.72	6390.84	7780.74
LZO	7989.70	33717.03	9429.92	6045.36	7772.44
RLE	9599.31	473270.61	34433.47	6336.51	7837.60
Z-Standard	8006.25	34914.99	9714.97	6023.48	<u>7758.87</u>
DeepMapping	5454.34	10511.73	2351.74	5686.15	5097.88

5.4.3 Latency. In Tables 3 and 4, we consider the end-to-end query latency for TPC-H and TPC-DS benchmarks, for different scale sizes and for different numbers of queries. As we see in these two tables, DeepMapping consistently outperforms the competitors in terms of query latency, especially when the data size and the number of queries to be processed get larger. Interestingly, we see that, for several of the competitors, the need to decompress data

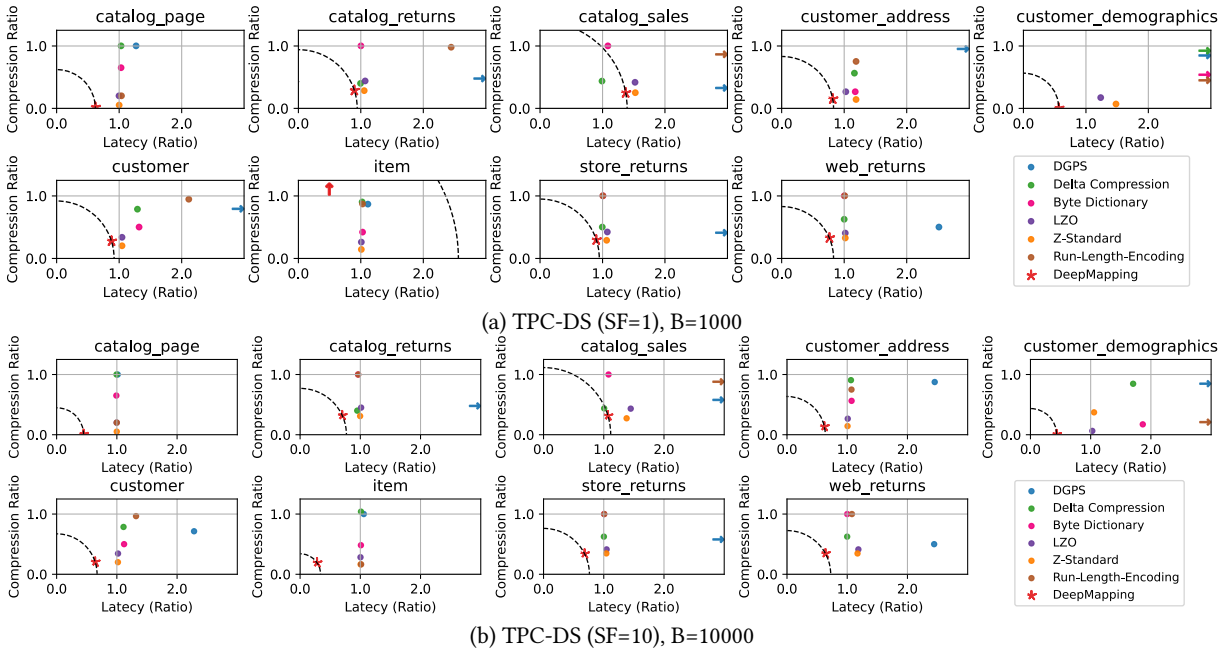


Figure 8: Trade-off between compression ratio and lookup performance in TPC-DS (SF=1 vs. 10), B=1000 and 10000 – Annotations are explained in the footnote ³

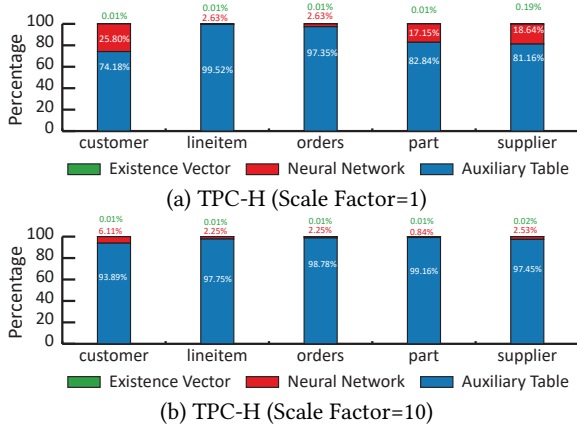


Figure 9: DeepMapping storage breakdown for TPC-H⁵

will significantly damage the lookup performance compared to the the uncompressed baseline. In contrast, DeepMapping consistently outperforms the uncompressed key-value map, providing up to 3× query speedup against the uncompressed baseline.

5.4.4 Latency- vs. Memory- Optimized Validation. Note that DeepMapping needs to decompress necessary partitions of the auxiliary quality assurance table, however, in most cases this does not cause significant overhead as illustrated in Figure 11. Moreover, in the default latency-optimized validation approach, as the number of queries increases, the relative overhead of the decompression process becomes significantly smaller. As we see in Table 5 memory-optimized validation strategy can significantly reduce peak memory consumption, but as we see in Table 6, this comes with additional latency due to reduced partition re-use, rendering the latency of DeepMapping second to the Uncompressed strategy. Nevertheless,

Table 4: Comparison of the end-end lookup latency of using different compression mechanisms on the TPC-DS (ms)

CP: catalog_page; CR: catalog_returns; CS: catalog_sales
CA: customer_address; C: customer; I: item; SR: store_returns; WR: web_returns

Lookup time (ms), Scale Factor = 1, B=1000										
Methods	CP	CR	CS	CA	CD	C	I	SR	WR	
Uncompressed	75.38	79.03	83.35	78.00	106.64	79.42	70.40	79.24	77.31	
DGPS	95.83	472.49	3487.51	331.38	6152.58	295.83	78.32	637.43	194.45	
DComp	77.63	78.65	82.66	90.76	784.43	102.75	71.90	78.95	77.25	
Byte Dictionary	77.76	79.19	90.49	91.74	896.58	104.81	72.41	79.85	77.44	
LZ0	75.25	84.43	126.81	79.99	131.98	83.06	70.99	85.37	78.60	
RLE	78.19	193.22	320.09	92.75	3230.96	167.85	72.28	79.62	77.93	
Z-Standard	75.37	83.33	127.01	92.75	157.91	83.16	70.99	84.45	78.69	
DeepMapping	46.76	70.88	114.16	63.65	60.39	69.69	39.72	71.34	59.08	

Lookup time (ms), Scale Factor = 1, B=10000										
Methods	CP	CR	CS	CA	CD	customer	item	SR	WR	
Uncompressed	747.58	780.71	794.22	774.02	858.34	784.33	702.85	785.62	769.91	
DGPS	761.71	1173.40	4184.99	1021.34	6877.37	1002.94	704.42	1340.24	885.46	
DComp	746.49	780.14	792.55	788.20	1533.94	811.80	705.55	784.73	771.01	
Byte Dictionary	745.35	778.65	800.66	785.26	1642.52	808.50	705.95	785.25	771.82	
LZ0	746.02	784.75	841.52	777.44	883.04	788.75	704.87	792.40	772.44	
RLE	748.11	895.81	1027.72	787.41	3982.76	904.26	705.16	786.39	775.49	
Z-Standard	746.39	786.77	837.04	773.83	906.43	789.25	704.07	791.44	773.10	
DeepMapping	381.46	530.10	581.26	504.70	385.52	520.81	208.81	537.33	502.81	

Lookup time (ms), Scale Factor = 10, B=10000										
Methods	CP	CR	CS	CA	CD	customer	item	SR	WR	
Uncompressed	769.60	849.74	950.64	835.93	899.43	845.13	756.99	846.69	839.71	
DGPS	780.52	4597.68	36191.30	2050.36	7014.34	1928.63	800.75	5772.81	2051.76	
DComp	765.15	806.50	956.98	887.73	1533.43	938.49	765.34	848.28	839.03	
Byte Dictionary	763.09	818.28	1026.09	896.52	1677.60	946.59	764.58	852.16	839.64	
LZ0	767.01	861.33	1376.16	843.33	923.74	861.36	759.35	886.67	995.36	
RLE	767.97	821.04	3943.79	895.21	4000.94	1114.41	767.04	853.42	905.34	
Z-Standard	768.49	847.11	1311.27	840.66	949.75	860.00	760.66	882.83	983.52	
DeepMapping	344.25	594.85	1017.28	518.57	390.96	540.63	213.45	577.12	536.48	

the overall latency is still competitive and is the best among all compression baselines even under memory-optimized validation.

5.4.5 Data Modifications (insert/update/delete). In order to investigate the performance of DeepMapping for data manipulation operations, we reuse the synthetic dataset that samples key-value mappings with low/high correlation of different sizes, 100M, 1GB, 10GB from the TPC-H and TPC-DS benchmarks. We then compare the storage and latency ratios against uncompressed data and Z-standard, which is the best baseline competitor based on the

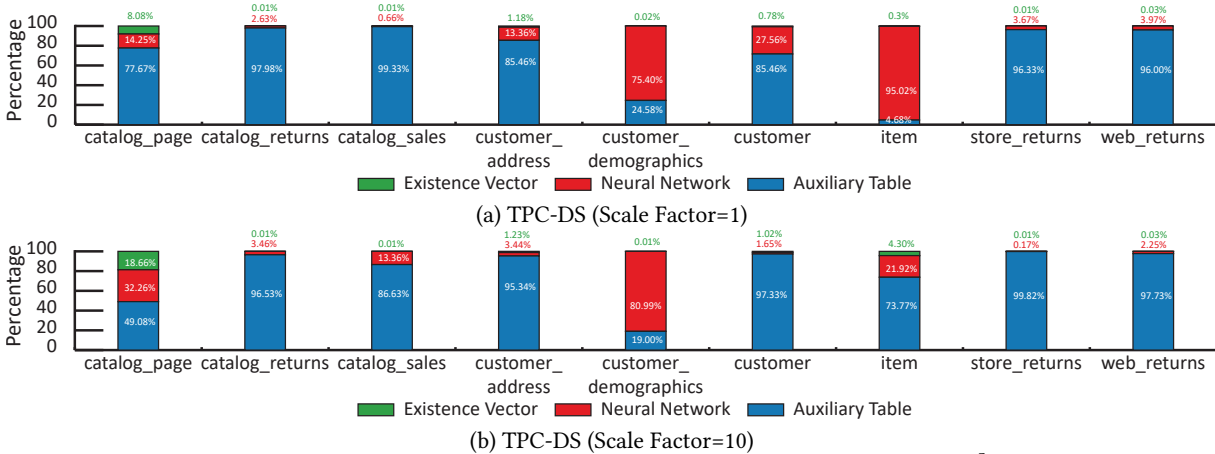


Figure 10: DeepMapping storage breakdown for TPC-DS benchmark⁵

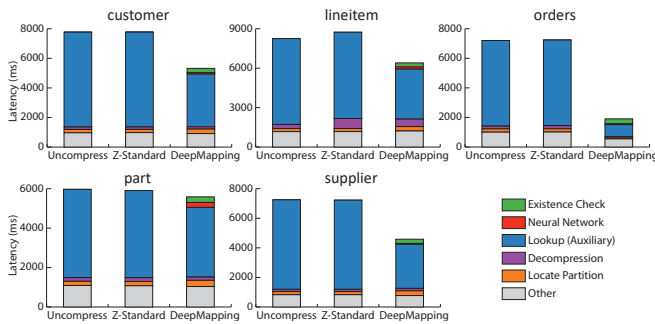


Figure 11: Breakdown of the end-end latency for TPC-H, SF=1, B=100,000

Table 5: Comparison of the online memory usage for memory- and latency-optimized validation strategies (100,000 look-ups on TPC-H dataset)

Peak Memory Usage (MB) Scale Factor: 10, B=10000 (Memory Optimized)					
Methods	customer	lineitem	orders	part	supplier
Uncompressed	2.00	2.00	0.50	2.00	1.53
DGPC	2.25	2.07	0.55	2.13	1.91
DComp	1.50	1.14	0.33	1.25	1.53
Byte Dictionary	1.56	1.25	0.35	1.34	1.53
LZO	1.31	1.24	0.32	1.35	1.07
RLE	1.26	1.18	0.28	1.23	1.00
Z-Standard	2.00	1.82	0.46	2.00	1.53
DeepMapping	1.46	8.38	7.43	1.56	0.96

Peak Memory Usage (MB) Scale Factor: 10, B=10000 (Latency Optimized)					
Methods	customer	lineitem	orders	part	supplier
Uncompressed	23.78	3077.30	343.49	62.00	1.53
DGPC	24.00	3077.58	286.13	62.15	1.91
DComp	23.11	3076.65	343.29	61.13	1.14
Byte Dictionary	23.39	3076.78	343.35	61.34	1.53
LZO	23.17	3076.77	343.32	61.33	1.07
RLE	23.12	3076.73	343.27	61.23	1.00
Z-Standard	23.78	3077.18	343.45	62.00	1.53
DeepMapping	17.22	1831.82	156.47	38.56	0.96

results presented so far. We implement modifications as follows: (a) For inserts, we use 90% of the data as the base table and add

Table 6: Comparison of the end-end data lookup latency under Run-Time Memory Optimized Strategy (TPC-H dataset)

Methods	Lookup time (ms) Scale Factor: 10, B=10000 (Memory Optimized)				
	customer	lineitem	orders	part	supplier
Uncompressed	814.19	3110.93	1192.43	595.15	782.23
DGPC	15529.31	1638703.09	122227.12	56032.25	956.50
DComp	2585.43	178523.72	24509.81	4461.40	784.57
Byte Dictionary	2656.47	194170.69	26218.98	4750.20	785.02
LZO	1016.11	24860.52	2916.24	1146.79	790.53
RLE	994.27	26380.77	3204.84	981.73	788.60
Z-Standard	2626.63	440078.12	27847.48	4640.07	791.04
DeepMapping	706.15	18626.35	2082.57	926.43	522.48

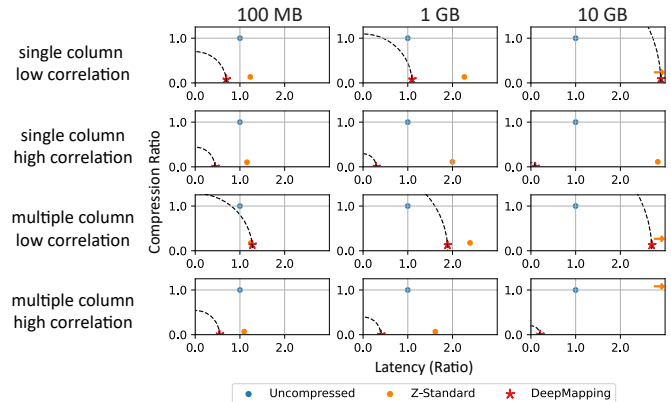


Figure 12: Size vs. latency ratio for insert operations—Annotations are explained in the footnote³.

the remaining 10% data to the original dataset; (b) For updates, we randomly update 10% in the base table, with the 10% data put aside for this purpose. (c) For deletes, we use 100% of the data as the base table and randomly delete 10% data. As illustrated in Figures 12 through 14, for data modification operations, DeepMapping provides the best storage vs. latency trade-off and easily outperforms the closest competitor Z-standard. While uncompressed data performs faster in certain configurations with low correlation,

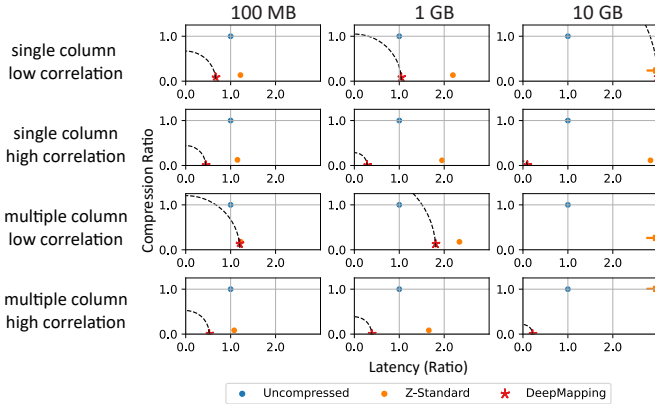


Figure 13: Size vs. latency ratio for update operations—Annotations are explained in the footnote ³.

DeepMapping provides better compression even in those cases and therefore is the preferred option in resource constrained settings.

5.4.6 MHAS - Multi-Task Hybrid Architecture Search. In this section, we further evaluate the effectiveness of our proposed MHAS algorithm. We use the TPC-H data set, with scale factor=1, with the configuration described in Sec. 5.1.

In Figure 15, we plot the compression ratio of the sampled models against the training process of the controller. As we see here, at the very beginning of the search stage, there is a "flat" region where the compression ratio is not yet decreasing – this is because, at the early stages, the sampled models are not yet capable to memorize the data. In fact, at this stage, the size of the data structure may be larger than the original data since a lot of the memorization work is left to the auxiliary table. As the controller training proceeds, however, the sampled models are quickly getting better at memorizing the data and the compression ratio improves significantly.

Finally, Figure 16 illustrates how the compression ratio vs. latency trade-off evolves during the search. In the figure, each dot corresponds to the performance of a sampled architecture and different colors correspond to the different stages of the search. As we see in this figure, initially, samples may cover a large range indicating that the model search has not stabilized; as the search progresses, however, the samples start clustering in an increasingly shrinking region of the trade-off space, illustrating the effectiveness of the MHAS strategy proposed in this paper.

6 CONCLUSIONS AND FUTURE WORKS

In this paper, we presented DeepMapping, which utilizes a hybrid architecture. It uses a lightweight auxiliary data structure to augment neural network models for better exploiting the memorization, compressibility, and GPU acceleration opportunities brought by deep learning *without any accuracy loss*. It also includes a novel multi-task hybrid architecture search strategy, MHAS. While existing AutoML strategies pursue high accuracy or small size of the model, MHAS targets minimizing the overall compression ratio of the entire hybrid architecture. MHAS automatically balances the numbers of shared and private layers (for each attribute) in the search space. Our experimental results, reported in the previous sections, show that DeepMapping strikes significantly better

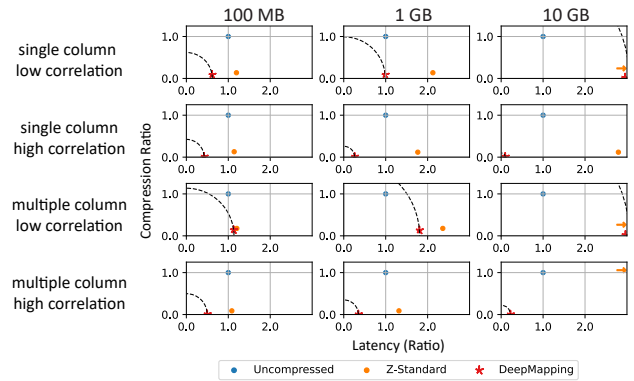


Figure 14: Size vs. latency ratio for delete operations—Annotations are explained in the footnote ³.

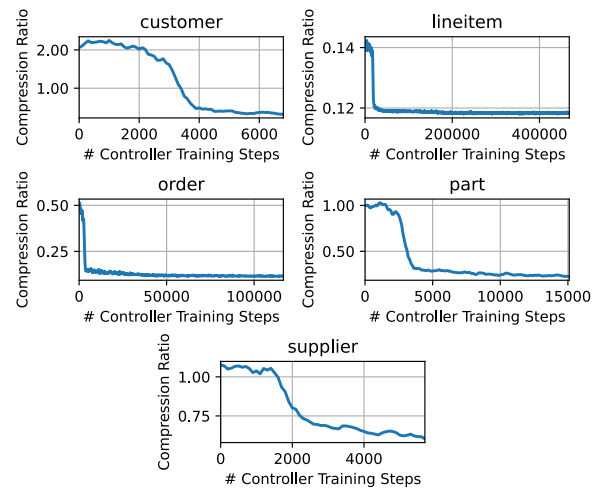


Figure 15: Compression ratios during MHAS (TPC-H, scale = 1; plots smoothed with running average window of 500)

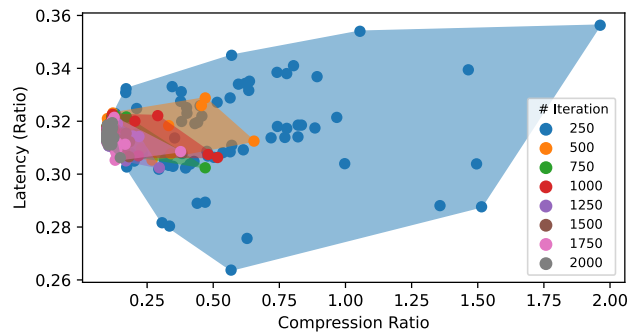


Figure 16: Progression of compression ratio vs. latency trade-off during MHAS search process (TPC-H part table, scale = 1; each dot corresponds to a sampled architecture and different colors correspond to different search stage)

trade-offs among query latency and storage efficiency for categorical and integer data, compared to state-of-art lossless compression techniques.

The proposed DeepMapping abstraction can readily facilitate various database problems that rely on the key-value data, such as hash maps that are used in hash-based join and aggregation,

and key-value stores, in resource constrained settings, such as edge computing and in-memory computing. Future work will include exploring the approach for scenarios that involve continuous numerical attributes and more complex multi-table queries.

REFERENCES

- [1] [n. d.]. Byte-dictionary encoding. https://docs.aws.amazon.com/redshift/latest/dg/c_byte_dictionary_encoding.html.
- [2] [n. d.]. Delta Encoding. https://en.wikipedia.org/wiki/Delta_encoding.
- [3] [n. d.]. LZ0 real-time data compression library. <http://www.oberhumer.com/opensource/lzo/>.
- [4] [n. d.]. Python bindings for the LZ0 data compression library. <https://pypi.org/project/python-lzo/>.
- [5] [n. d.]. TensorFlow Hub. <https://tfhub.dev/>.
- [6] [n. d.]. TPC-DS Benchmark. <https://www.tpc.org/tpcds/>.
- [7] [n. d.]. TPC-H Benchmark. <https://www.tpc.org/tpch/>.
- [8] [n. d.]. ZSTD Bindings for Python. <https://pypi.org/project/zstd/>.
- [9] James Bergstra, Rémi Bardenet, Yoshua Bengio, and Balázs Kégl. 2011. Algorithms for hyper-parameter optimization. *Advances in neural information processing systems* 24 (2011).
- [10] Yann Collet and Murray Kucherawy. 2021. Zstandard Compression and the 'application/zstd' Media Type. RFC 8878. <https://doi.org/10.17487/RFC8878>
- [11] Alexis Conneau, Kartikay Khandelwal, Naman Goyal, Vishrav Chaudhary, Guillaume Wenzek, Francisco Guzmán, Edouard Grave, Myle Ott, Luke Zettlemoyer, and Veselin Stoyanov. 2019. Unsupervised cross-lingual representation learning at scale. *arXiv preprint arXiv:1911.02116* (2019).
- [12] George Cybenko. 1989. Approximation by superpositions of a sigmoidal function. *Mathematics of control, signals and systems* 2, 4 (1989), 303–314.
- [13] Jialin Ding, Umar Farooq Minhas, Jia Yu, Chi Wang, Jaeyoung Do, Yinan Li, Hantian Zhang, Badrish Chandramouli, Johannes Gehrke, Donald Kossmann, et al. 2020. ALEX: an updatable adaptive learned index. In *Proceedings of the 2020 ACM SIGMOD International Conference on Management of Data*. 969–984.
- [14] Jialin Ding, Vikram Nathan, Mohammad Alizadeh, and Tim Kraska. 2020. Tsunami: A learned multi-dimensional index for correlated data and skewed workloads. *arXiv preprint arXiv:2006.13282* (2020).
- [15] Paolo Ferragina and Giorgio Vinciguerra. 2020. The PGM-index: a fully-dynamic compressed learned index with provable worst-case bounds. *Proceedings of the VLDB Endowment* 13, 8 (2020), 1162–1175.
- [16] Solomon Golomb. 1966. Run-length encodings (corresp.). *IEEE transactions on information theory* 12, 3 (1966), 399–401.
- [17] Tim Gubner, Viktor Leis, and Peter Boncz. 2021. Optimistically Compressed Hash Tables & Strings in the USSR. *ACM SIGMOD Record* 50, 1 (2021), 60–67.
- [18] Zichao Guo, Xiangyu Zhang, Haoyuan Mu, Wen Heng, Zechun Liu, Yichen Wei, and Jian Sun. 2020. Single path one-shot neural architecture search with uniform sampling. In *European conference on computer vision*. Springer, 544–560.
- [19] Brian Hentschel, Utku Sirin, and Stratos Idreos. 2022. Entropy-Learned Hashing: 10x Faster Hashing with Controllable Uniformity. SIGMOD.
- [20] Benjamin Hilprecht, Andreas Schmidt, Moritz Kulesa, Alejandro Molina, Kristian Kersting, and Carsten Binnig. 2019. Deepdb: Learn from data, not from queries! *arXiv preprint arXiv:1909.00607* (2019).
- [21] Geoffrey E Hinton, Peter Dayan, Brendan J Frey, and Radford M Neal. 1995. The "wake-sleep" algorithm for unsupervised neural networks. *Science* 268, 5214 (1995), 1158–1161.
- [22] Kurt Hornik, Maxwell Stinchcombe, and Halbert White. 1989. Multilayer feedforward networks are universal approximators. *Neural networks* 2, 5 (1989), 359–366.
- [23] Guang-Bin Huang. 2003. Learning capability and storage capacity of two-hidden-layer feedforward networks. *IEEE transactions on neural networks* 14, 2 (2003), 274–281.
- [24] Friso Kingma, Pieter Abbeel, and Jonathan Ho. 2019. Bit-swap: Recursive bits-back coding for lossless compression with hierarchical latent variables. In *International Conference on Machine Learning*. PMLR, 3408–3417.
- [25] Andreas Kipf, Ryan Marcus, Alexander van Renen, Mihail Stoian, Alfons Kemper, Tim Kraska, and Thomas Neumann. 2020. RadixSpline: a single-pass learned index. In *Proceedings of the third international workshop on exploiting artificial intelligence techniques for data management*. 1–5.
- [26] Tim Kraska, Alex Beutel, Ed H Chi, Jeffrey Dean, and Neoklis Polyzotis. 2018. The case for learned index structures. In *Proceedings of the 2018 international conference on management of data*. 489–504.
- [27] Liam Li and Ameet Talwalkar. 2020. Random search and reproducibility for neural architecture search. In *Uncertainty in artificial intelligence*. PMLR, 367–377.
- [28] Pengfei Li, Hua Lu, Qian Zheng, Long Yang, and Gang Pan. 2020. LISA: A learned index structure for spatial data. In *Proceedings of the 2020 ACM SIGMOD international conference on management of data*. 2119–2133.
- [29] Hanxiao Liu, Karen Simonyan, and Yiming Yang. 2018. Darts: Differentiable architecture search. *arXiv preprint arXiv:1806.09055* (2018).
- [30] Yuqiao Liu, Yanan Sun, Bing Xue, Mengjie Zhang, Gary G Yen, and Kay Chen Tan. 2021. A survey on evolutionary neural architecture search. *IEEE transactions on neural networks and learning systems* (2021).
- [31] Minh-Thang Luong, Quoc V Le, Ilya Sutskever, Oriol Vinyals, and Lukasz Kaiser. 2015. Multi-task sequence to sequence learning. *arXiv preprint arXiv:1511.06114* (2015).
- [32] Qingzhi Ma and Peter Triantafillou. 2019. Dbest: Revisiting approximate query processing engines with machine learning models. In *Proceedings of the 2019 International Conference on Management of Data*. 1553–1570.
- [33] Michael McCloskey and Neal J Cohen. 1989. Catastrophic interference in connectionist networks: The sequential learning problem. In *Psychology of learning and motivation*. Vol. 24. Elsevier, 109–165.
- [34] Fabian Mentzer, Luc Van Gool, and Michael Tschannen. 2020. Learning better lossless compression using lossy compression. In *Proceedings of the IEEE/CVF Conference on Computer Vision and Pattern Recognition*. 6638–6647.
- [35] Barzan Mozafari. 2016. When Should Approximate Query Processing Be Used? (2016). <http://highscalability.com/blog/2016/2/25/when-should-approximate-query-processing-be-used.html>
- [36] Vikram Nathan, Jialin Ding, Mohammad Alizadeh, and Tim Kraska. 2020. Learning multi-dimensional indexes. In *Proceedings of the 2020 ACM SIGMOD international conference on management of data*. 985–1000.
- [37] Varun Pandey, Alexander van Renen, Andreas Kipf, Ibrahim Sabek, Jialin Ding, and Alfons Kemper. 2020. The case for learned spatial indexes. *arXiv preprint arXiv:2008.10349* (2020).
- [38] Jay M Patel and Jay M Patel. 2020. Introduction to common crawl datasets. *Getting Structured Data from the Internet: Running Web Crawlers/Scrapers on a Big Data Production Scale* (2020), 277–324.
- [39] Hieu Pham, Melody Guan, Barret Zoph, Quoc Le, and Jeff Dean. 2018. Efficient neural architecture search via parameters sharing. In *International conference on machine learning*. PMLR, 4095–4104.
- [40] Jianzhong Qi, Guanli Liu, Christian S Jensen, and Lars Kulik. 2020. Effectively learning spatial indices. *Proceedings of the VLDB Endowment* 13, 12 (2020), 2341–2354.
- [41] Esteban Real, Alok Aggarwal, Yanping Huang, and Quoc V Le. 2019. Regularized evolution for image classifier architecture search. In *Proceedings of the aaai conference on artificial intelligence*, Vol. 33. 4780–4789.
- [42] Ibrahim Sabek and Tim Kraska. 2021. The Case for Learned In-Memory Joins. *arXiv preprint arXiv:2111.08824* (2021).
- [43] Ibrahim Sabek, Kapil Vaidya, Dominik Horn, Andreas Kipf, and Tim Kraska. 2021. When Are Learned Models Better Than Hash Functions? *arXiv preprint arXiv:2107.01464* (2021).
- [44] Ibrahim Sabek, Kapil Vaidya, Dominik Horn, Andreas Kipf, Michael Mitzenmacher, and Tim Kraska. 2022. Can Learned Models Replace Hash Functions? *Proceedings of the VLDB Endowment* 16, 3 (2022), 532–545.
- [45] Ali Sharif Razavian, Hossein Azizpour, Josephine Sullivan, and Stefan Carlsson. 2014. CNN features off-the-shelf: an astounding baseline for recognition. In *Proceedings of the IEEE conference on computer vision and pattern recognition workshops*. 806–813.
- [46] Yibo Yang, Robert Bamler, and Stephan Mandt. 2020. Improving inference for neural image compression. *Advances in Neural Information Processing Systems* 33 (2020), 573–584.
- [47] Sepanta Zeighami, Ritesh Ahuja, Gabriel Ghinita, and Cyrus Shahabi. 2022. A Neural Database for Differentially Private Spatial Range Queries. *Proc. VLDB Endow.* 15, 5 (2022), 1066–1078. <https://www.vldb.org/pvldb/vol15/p1066-zeighami.pdf>
- [48] Sepanta Zeighami and Cyrus Shahabi. 2021. NeuroDB: A Neural Network Framework for Answering Range Aggregate Queries and Beyond. *arXiv preprint arXiv:2107.04922* (2021).
- [49] Sepanta Zeighami, Cyrus Shahabi, and Vatsal Sharan. 2022. NeuroSketch: Fast and Approximate Evaluation of Range Aggregate Queries with Neural Networks. *arXiv preprint arXiv:2211.10832* (2022).
- [50] Barret Zoph and Quoc V Le. 2016. Neural architecture search with reinforcement learning. *arXiv preprint arXiv:1611.01578* (2016).
- [51] Barret Zoph, Vijay Vasudevan, Jonathon Shlens, and Quoc V Le. 2018. Learning transferable architectures for scalable image recognition. In *Proceedings of the IEEE conference on computer vision and pattern recognition*. 8697–8710.
- [52] Barret Zoph, Deniz Yuret, Jonathan May, and Kevin Knight. 2016. Transfer learning for low-resource neural machine translation. *arXiv preprint arXiv:1604.02201* (2016).
- [53] Jia Zou. 2021. Using Deep Learning Models to Replace Large Materialized Views in Relational Database. In *11th Conference on Innovative Data Systems Research, CIDR 2021, Virtual Event, January 11–15, 2021, Online Proceedings*. www.cidrdb.org. http://cidrdb.org/cidr2021/papers/cidr2021_abstract05.pdf